

❸Impact of Lateral Boundary Conditions on Regional Analyses

KAMEL CHIKHAR AND PIERRE GAUTHIER

Étude et Simulation du Climat à l'Échelle Régionale Centre, University of Québec at Montréal, Montréal, Québec, Canada

(Manuscript received 28 June 2016, in final form 4 December 2016)

ABSTRACT

Regional and global climate models are usually validated by comparison to derived observations or reanalyses. Using a model in data assimilation results in a direct comparison to observations to produce its own analyses that may reveal systematic errors. In this study, regional analyses over North America are produced based on the fifth-generation Canadian Regional Climate Model (CRCM5) combined with the variational data assimilation system of the Meteorological Service of Canada (MSC). CRCM5 is driven at its boundaries by global analyses from ERA-Interim or produced with the global configuration of the CRCM5. Assimilation cycles for the months of January and July 2011 revealed systematic errors in winter through large values in the mean analysis increments. This bias is attributed to the coupling of the lateral boundary conditions of the regional model with the driving data particularly over the northern boundary where a rapidly changing large-scale circulation created significant cross-boundary flows. Increasing the time frequency of the lateral driving and applying a large-scale spectral nudging significantly improved the circulation through the lateral boundaries, which translated in a much better agreement with observations.

1. Introduction

When used in data assimilation, a model is constantly compared to observations. Based on statistical estimation principles, a short-term model forecast from the previous analysis is drawn toward the observations through the assimilation process that builds a correction to the background state, the analysis increment, which should in principle be unbiased. That is, in a bias free data assimilation system, the analysis increment averaged over a sufficiently large ensemble should be close to zero (Dee 2005). Therefore, a systematic correction is indicative of a bias associated with error in either the observations or the background state itself or both. On the other hand, Rodwell and Palmer (2007, hereafter RP07) pointed out that a bias in the analysis increment corresponds to an opposite systematic physical tendency observed in the first time steps of a 6-h forecast. A diagnostic based on tendencies provides also useful information to diagnose the fast-acting processes of the

model. The total tendency is the sum of the tendencies from each of the physical processes and the dynamics. It is expected that at any location, the total tendency and the analysis increments should average to zero over a large number of cases (RP07). Because it is constantly drawn toward the observations by the assimilation, the model's forecast tends to restore its own equilibrium during the short-term integration to produce the background state. These diagnostics are therefore revealing imbalances associated with the adjustment from the observed climatology to that of the model. This is why it is necessary that the model we want to assess be the one used to produce its own analyses. This suggests that data assimilation could be valuable even for climate models as a diagnostic approach to test, for example, different configurations to prevent the emergence of spurious internal variability associated with unbalanced physics in the model. A detailed explanation of the initial tendency diagnostic approach can be found in RP07 and Chikhar and Gauthier (2014). The latter evaluated the Global Environmental Multiscale (GEM) (Côté et al. 1998) model and the fifth-generation Canadian Regional Climate Model (CRCM5) (Zadra et al. 2008) by analyzing their initial dynamical balance based on the initial tendency diagnostic. It is important to mention that Chikhar and Gauthier (2014) used existing analyses, namely analyses from the Meteorological Service of

❸ Denotes content that is immediately available upon publication as open access.

Corresponding author e-mail: Kamel Chikhar, chikhar@sca.uqam.ca

Canada (MSC) (Gauthier et al. 2007; Laroche et al. 2007) and those of ERA-Interim (Dee et al. 2011), with the objective of studying the sensitivity to initial and boundary conditions. They showed that the analyses have a significant impact on the model and can lead to the emergence of a bias. On the other hand, a bias in the model can be caused by the lateral driving, and Chikhar and Gauthier (2015) used physical and dynamical tendencies to detect a sensitivity of the CRCM5 to changes in the lateral boundary conditions.

These studies and others (e.g., Rodwell and Jung 2008) revealed the usefulness of the initial tendencies in model development and evaluation. This suggested using the CRCM5 within an assimilation system to assess a model through information brought in by the assimilation and the initial tendency diagnostic. This is the essential motivation of the work presented here. Taking advantage of the fact that the CRCM5 is very close to the limited-area regional model of MSC, GEM-LAM (Mailhot et al. 2006), used to produce regional analyses (Caron et al. 2015), it was technically possible to use the CRCM5 instead of the GEM-LAM in data assimilation and therefore, to benefit from the immense work done to validate the system for the large volume of assimilated data. Validating a model in this context is a long process, and this approach avoided many difficulties that arise when building a data assimilation system from scratch (e.g., quality control of the observations, detailed study of each observation operator, tuning of the error statistics). The objective of the study was to see first if the system could be cycled in time without drifting. Moreover, it was envisioned that the analysis increments and the physical tendencies on top of the data monitoring could help us pinpoint the source of problems if any.

In collaboration with Environment and Climate Change Canada (ECCC), the MSC regional ensemble-variational data assimilation system (EnVar) (Buehner et al. 2015; Caron et al. 2015) was adapted to use the CRCM5 in the assimilation of all observations currently used at MSC. However, producing regional analyses in a fully cycled assimilation system gives rise to difficulties associated with the way the regional model is driven at its lateral boundaries. The lateral driving can induce important contrasts between the driving data and the regional model forecast due to many factors such as, for example, differences in spatial resolution and physical parameterizations used in the driving and driven models (Warner et al. 1997; Scinocca et al. 2016). Moreover, it is well known that regional models do not represent well the large-scale circulation because of their limited integration domain (Kanamaru and Kanamitsu 2007; Scinocca et al. 2016). In addition, the error in the

forecast of the regional model can be exacerbated when the lateral boundary is located where a fast-moving synoptic circulation creates rapidly changing cross-boundary flows (Denis et al. 2002). As a result, the background state provided to the assimilation system could then be very poor and even unrealistic in the vicinity of the nesting zone.

In many regional assimilation systems, the regional model is driven by its global version or global reanalyses (e.g., Fillion et al. 2010; Mesinger et al. 2006). In our study, the lateral driving issue will be examined using ERA-Interim reanalyses as well as global analyses based on the GEMCLIM model, the CRCM5 global version. This will allow us to test their compatibility with the regional model and also investigate different nesting procedures.

The paper is organized as follows. In section 2, the experimental framework is presented describing the assimilation system as well as the model used. A preliminary evaluation of the regional assimilation is presented in section 3. A deeper investigation is presented in sections 4–7 to address the nesting procedure issue and establish an adequate lateral driving strategy. A verification of the regional assimilation system in its adopted settings is presented in section 8. Finally, conclusions are given in section 9.

2. The regional assimilation system: Design and experimental framework

The configuration of the CRCM5 used is the same as that described in Chikhar and Gauthier (2014). Namely, it uses a terrain-following vertical coordinate (Laprise 1992) with 80 levels up to 0.1 hPa. The horizontal resolution is ~ 20 km with a time step of 10 min. In our system, the boundary conditions are applied in a band along the boundary of the domain, the width of which comprises 20 grid points. The outermost 10 grid points are used as upstream data for the semi-Lagrangian interpolation while the next 10 grid points delimit the blending zone where the model solution is relaxed to the driving data using a method introduced by Davies (1976). The background states are forecasts from the model valid at every time step for a 6-h interval centered on the time of the analysis which is either 0000, 0600, 1200, or 1800 UTC. The domain used in the experimentation (see Fig. 1) is the same as that used in the Coordinated Regional Climate Downscaling Experiment (CORDEX) over North America (Šeparović et al. 2013).

The assimilation system is based on the four-dimensional ensemble-variational data assimilation (4DEnVar) recently implemented at MSC for

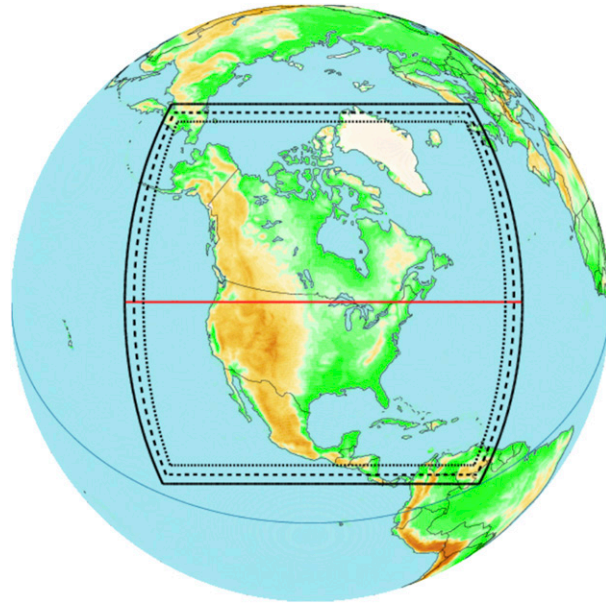


FIG. 1. The domain used in the experimental regional assimilation system. The inner thin dotted lines indicate the free model zone limit while the area between the two dotted lines represents the blending region. The red line indicates the grid equator.

deterministic weather prediction (Buehner et al. 2015; Caron et al. 2015). The 4DEnVar is an incremental variational assimilation system based on the use of hybrid background error covariances with a weighted average of the static covariances B_{nmc} formulation, used in the previous 4DVar and 3DVar systems, and a flow-dependent 4D ensemble covariances B_{ens} obtained from the ensemble Kalman filter assimilation system also used at MSC for its ensemble prediction system (Houtekamer et al. 2014). In our experiments, only the static covariances B_{nmc} were used, making in fact the 4DEnVar a 3DVar First Guess at Appropriate Time (FGAT). The static covariances were estimated from the global GEM model forecasts using the so-called NMC method (Parrish and Derber 1992). The minimization employs a quasi-Newton algorithm (Gilbert and Lemaréchal 1989) with 70 iterations, the first 5 iterations being done without the variational quality control (QC-Var) (Gauthier et al. 2003). The observations assimilated over a 6-h window are only those located within the model domain and include data from radiosondes, aircraft, surface land stations, buoys, ships, wind profilers, scatterometers, microwave and infrared satellite sounders and imagers, atmospheric motion vectors, and satellite-based GPS radio occultation. This assimilation system produces analysis increments over a 400×200 global grid corresponding to a resolution of ~ 100 km. These increments are then interpolated to the CRCM5

higher resolution (~ 20 km) over the model domain and added to the background state to produce the analysis. However, in the incremental formulation (Courtier et al. 1994; Gauthier et al. 2007), while using the model at its full resolution is essential to compare the background state to the observations, the filtering properties of the background error statistics only require that the analysis increment be at a coarser resolution. In Laroche et al. (1999), it is shown that the analysis increment produced at the full resolution is nearly identical to what is obtained by using the incremental formulation.

3. Evaluation of the regional assimilation system

Assimilation cycles have been completed for January and July 2011. The term cycle stands here for the process through which each analysis is used as initial conditions for the next forecast used as the background state in the assimilation that produces the next analysis. In each experiment, the assimilation was cycled for one week to allow a spinup of the assimilation and the regional model driven 6-hourly at its lateral boundaries by global analyses.

a. The mean analysis increments

The analysis increment $\delta\mathbf{x}_a = \mathbf{x}_a - \mathbf{x}_b$ is defined as the correction added to the background state \mathbf{x}_b to obtain the analysis \mathbf{x}_a . In absence of biases in the observation and background error, it is expected that the average of the analysis increments obtained during a one-month cycle should approximately vanish (Dee 2005). If not, this is an indication of the presence of systematic errors in the background, the observations, or both. Figure 2 shows the mean temperature analysis increment averaged over January and July 2011 at different vertical levels. In July (Fig. 2b), it is small over a large part of the domain except near the 100-hPa level where slightly positive mean increments are indicative of a cold bias in the background state. In January, however, significantly larger mean analysis increments are observed particularly over the northern Canadian archipelago at 100 and 250 hPa (Fig. 2a), but they decrease as we move toward lower levels.

These relatively large negative values in the mean analysis increments could be attributed to two possible causes. It could be that “weaknesses” in the model are causing a departure from the observations in those regions that would indicate that the model is too “warm” in the northern part of the domain. Or it could be that the observations in the region have a cold bias. Monitoring of the data represents the departures of observations with respect to forecasts, called the innovations $\text{OMF} = [\mathbf{y} - H(\mathbf{x}_b)]$, where \mathbf{y} is a vector representing all the observations, while H is the observation operator linking the model state to the observations. Similarly,

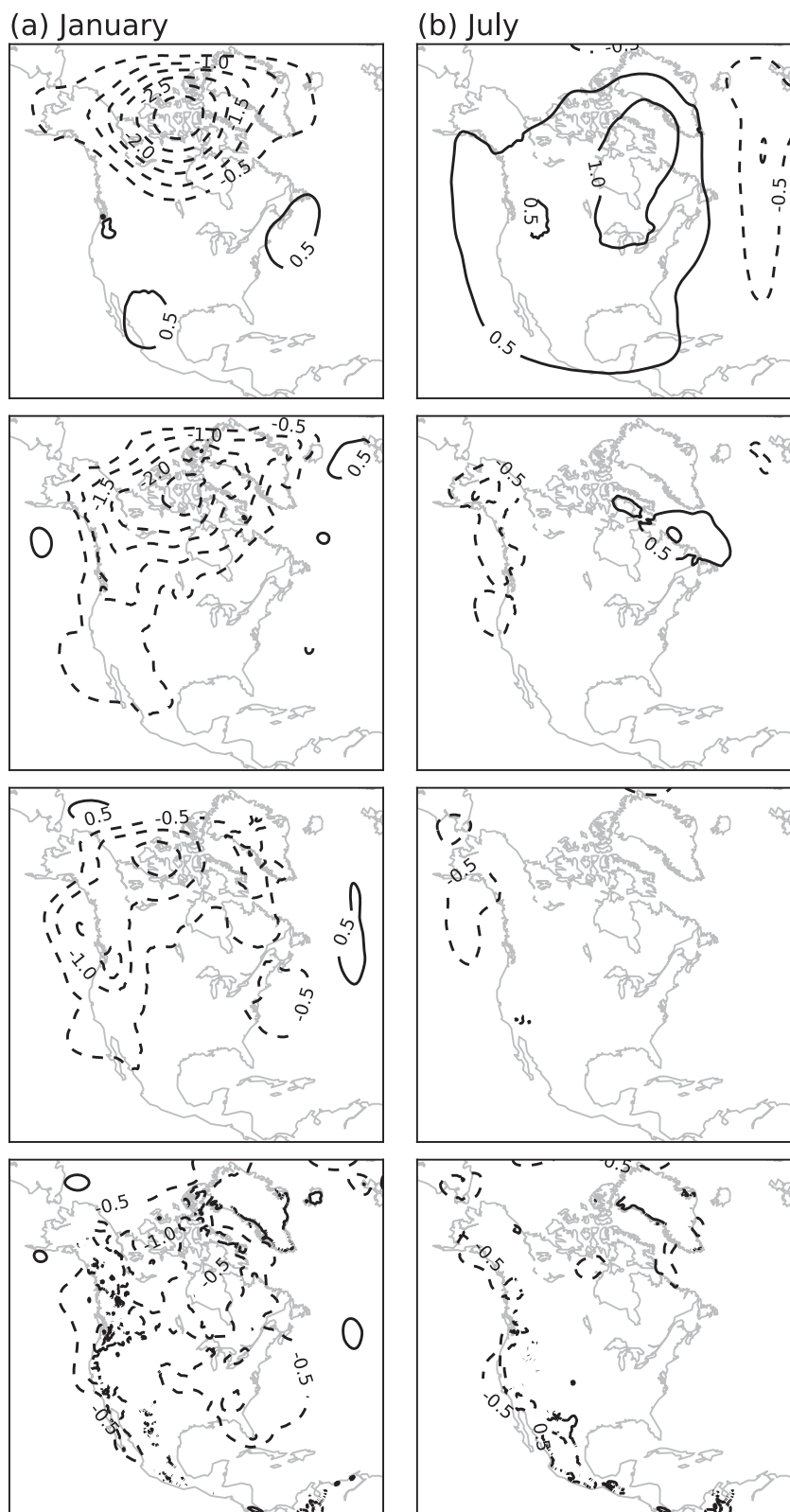


FIG. 2. Mean temperature increment ($^{\circ}$ C) from the analysis averaged over (a) January 2011 and (b) July 2011 for pressure levels (from top to bottom) 100, 250, 500, and 850 hPa.

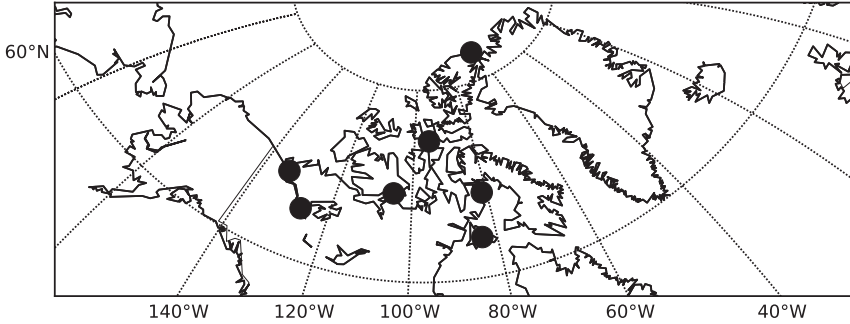


FIG. 3. Sounding stations used in the data monitoring indicated by black filled circles.

the analysis residuals $\text{OMA} = [\mathbf{y} - H(\mathbf{x}_a)]$ show the impact of the analysis, which is to draw the model state closer to the observations. At any analysis time, these are averaged by grouping all similar observations. One would expect that they would both average out to zero if the observations and background error were unbiased.

Figure 3 shows that there are a few radiosondes located in the region north of Canada in January where the anomalous mean analysis increment was observed (see Fig. 2). Figure 4a shows the temperature monitoring for all of the radiosondes in January, the OMF corresponding to the solid line and the OMA corresponding to the dotted line. The innovations present large values indicating a background departure from observations. The smaller values for the OMA compared to innovations indicate that the assimilation draws the background toward the observations. The values of the bias in the innovations can be lower than -8 K at times, which is abnormally large compared with the temperature observation error standard deviation ($\sim 1.4\text{ K}$). At all levels, the mean innovations remain negative meaning that the model is too warm compared to observations. This is particularly strong in the second half of the month and also stronger in the upper levels. This indicates that a significant portion of the mean bias in the analysis increment is related to the elevated bias between 15 and 25 January. The experiment was extended to the month of February, and the results indicate that the bias in the innovations subside only to reappear a few days later. Temperature observations from these soundings can be considered unbiased so that biases in the innovations point to problems with the model. In the summer case, Fig. 4b shows very small OMF and OMA indicating that the assimilation system is doing well, and the model forecast is also close to observations except at 100-hPa level where slightly positive OMF are observed.

b. Assimilation using only radiosonde data

In a new experiment performed over the month of January, only observations from radiosondes were

assimilated to rule out possible problems with the assimilation of satellite data over continents. The radiosonde observations are deemed unbiased and can be considered as a reference in our experiments. Radiosondes provide $\sim 20\,000$ temperature and wind data points at 0000 and 1200 UTC to the assimilation. The monitoring of the same radiosondes as those shown in Fig. 3 leads to similar results as those in Fig. 4a confirming that the large differences between the model and observations remain. This in our view ruled out the possibility that the observations were responsible for the large mean analysis increments observed in the northern part of the domain. If it is the model that causes such biases, a biased analysis increment would translate as a systematic physical tendency according to RP07.

4. Diagnostics based on initial tendencies

When an analysis used as initial conditions for the short-term forecast is used as the background state for the next assimilation, it may lead to dynamical imbalances and trigger a relaxation phase to restore the model's own equilibrium. In RP07, it is shown that the presence of a bias in the mean analysis increments creates a similar bias of the opposite sign in the total mean physical and dynamical tendencies associated with this systematic relaxation process. Considering the temperature analysis increments $\Delta T_a^{(n)}$ at the analysis time t_n for $n = 1, \dots, N$, with N being the number of analyses, it can be shown that

$$\begin{aligned}\overline{\Delta T_a} &= \frac{1}{N} \sum_{n=1}^N \Delta T_a^{(n)} \cong -\frac{\Delta t}{N} \sum_{n=1}^N \dot{T}^{(n)} \\ &= -\frac{\Delta t}{N} \sum_{n=1}^N \sum_{k=1}^p \dot{T}_k^{(n)} = -\Delta t \sum_{k=1}^p \overline{\dot{T}}_k,\end{aligned}$$

where $\dot{T}^{(n)}$ is the total tendency at the analysis time t_n , the index $k = 1, \dots, p$ represents the p physical and dynamical processes with $\dot{T}_k^{(n)}$ representing their

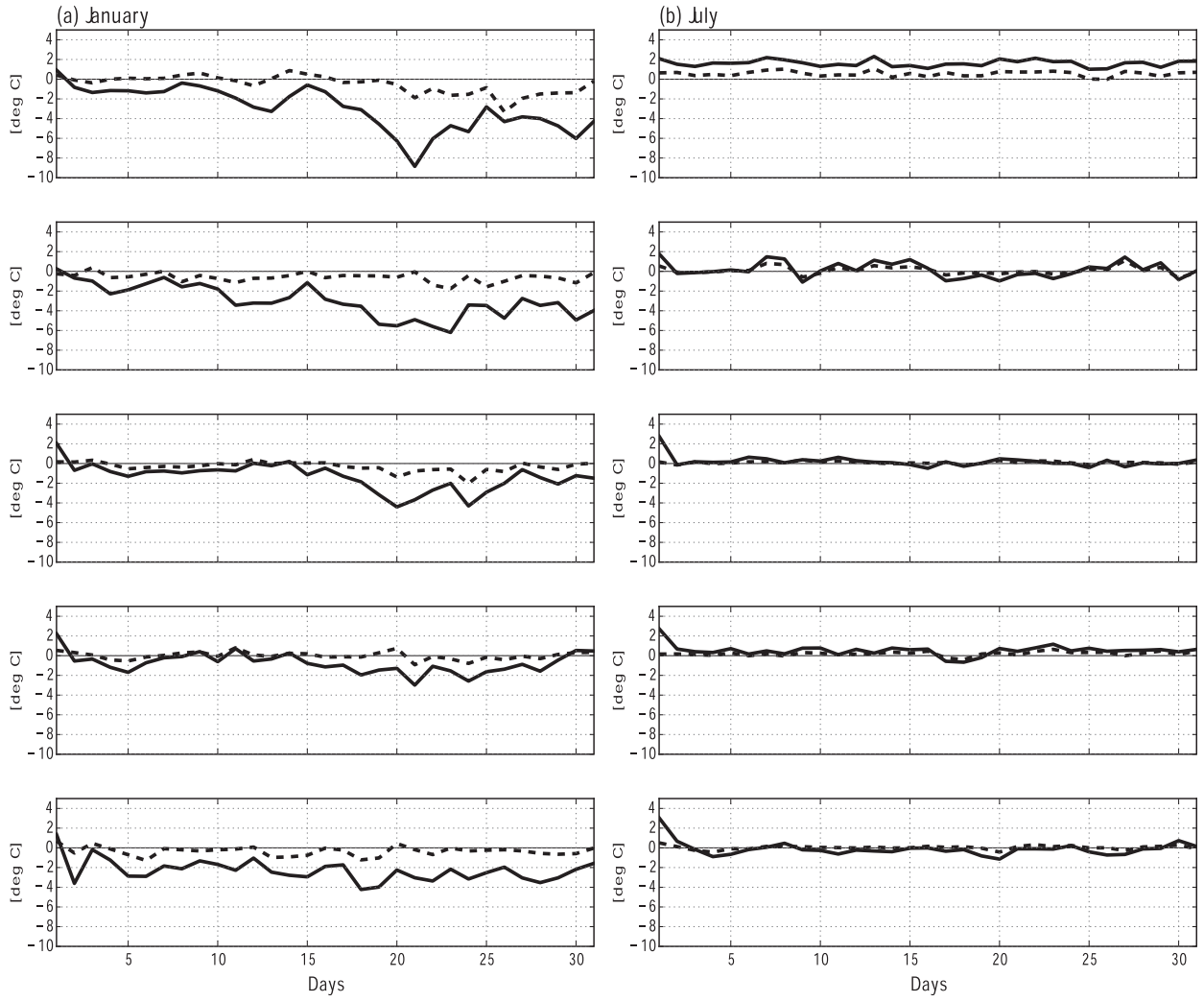


FIG. 4. Mean OMF (solid line) and OMA (dotted line) computed for temperature observations from soundings in northern Canada over the month of (left) January and (right) July 2011 at levels (from top to bottom) 100, 250, 500, 700, and 850 hPa. See text for OMF and OMA definitions.

individual tendencies, and the overbar stands for averaging over all the analysis times. More details can be found in RP07. An examination of the different components of the total tendency associated with the individual processes provides information that has been found useful in understanding the source of the bias of the analysis increment that may be associated with the model itself. In Chikhar and Gauthier (2014), these diagnostics were used to assess the impact of using third party analyses as initial conditions and/or boundary conditions in the CRCM5.

Since the mean analysis increments should average to zero over some period of time, the mean initial tendency averaged over a large number of forecasts should be close to zero as well for an unbiased model. Significant nonzero values are indicative of some imbalances and,

as argued in RP07, this provides a very useful diagnostic to study the impact of different model configurations. Applied to the mean initial tendency for temperature of the CRCM5, the total tendency includes components associated with convection, radiation, vertical diffusion, large-scale condensation, and dynamics.

A 6-h temporal average of tendencies for temperature were calculated for 6-h forecasts based on the analyses at 0000, 0600, 1200, and 1800 UTC for the month of January 2011. After spatially averaging over the free region of the model (i.e., excluding the blending zone), the profiles of the total temperature tendency were obtained together with those associated with the individual processes updating the temperature variable. Figure 5 shows a large positive systematic tendency at nearly all model levels from temperature advection (dynamics)

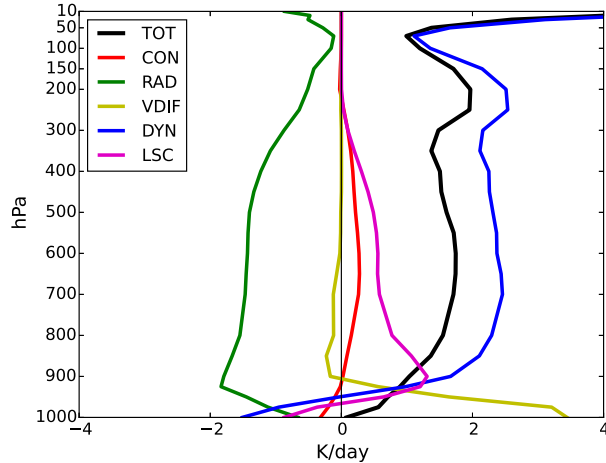


FIG. 5. Mean temperature initial systematic tendency (K day^{-1}) computed for the month of January 2011 and averaged over the free model zone. The different colors indicate the different processes involved: radiation (green), convection (red), large-scale condensation (magenta), vertical diffusion (brown), and advection (blue). The black line is the net tendency.

creating an excessive heating consistent with the large negative mean analysis increments observed in Fig. 2 required to bring the analysis closer to the observations. The initial mean temperature due to dynamics is

$$\overline{\left(\frac{\partial T}{\partial t}\right)}_{\text{adv.}} \approx -\mathbf{v} \cdot \nabla T,$$

where \mathbf{v} is the wind vector and ∇T , the temperature gradient. It corresponds to advection of temperature that, when averaged spatially over the domain, would be attributed to heat fluxes through the boundaries.

Figures 6a and 6b show the horizontal distribution of the mean initial tendency associated with dynamics at 100- and 250-hPa levels. Comparing this with Fig. 2, a large warming is observed exactly where there are negative mean analysis increments. This suggests the bias in the analysis increments is related to errors in the large-scale part of the flow.

So far the diagnostics based on the temperature tendencies have enabled us to relate the bias in the analysis increment to a particular process, advection, and in a particular region. Furthermore, Fig. 6c shows the time series of the tendency associated with advection averaged over the model's domain indicating that the systematic erroneous advection of temperature occurs between 9 and 21 January. This decreases afterward only to reappear later (between 25 and 30 January).

Figure 7 shows ERA-Interim reanalysis geopotential heights at 100 and 250 hPa, respectively, for 1800 UTC 22 January 2011. Figure 8 shows the corresponding

fields of the regional model, which shows a serious mismatch near the northern boundary and a more zonal and less meridional flow in the northwestern quadrant. This situation occurred several times during that month. The comparison clearly shows inconsistencies in the large-scale flow between the lateral boundary conditions (LBCs) and the regional model due to differences in evolution (Davies 2014). The model then becomes too warm as shown in the dynamics tendency in Fig. 5. In the assimilation, this problem leads to an important departure between the observations in the area and the background state defined by this forecast. The resulting analysis increment spreads the problem deeper in the interior of the domain according to the structure functions of the background error covariances.

In the current configuration of the CRCM5, the boundary conditions are provided by global analyses or forecasts at 6-h intervals that are linearly interpolated in time over the 6-h period. However, as discussed in Fillion et al. (2010) and Zhong et al. (2010), this may be revisited to better take into account the location of the boundaries, the size of the model's domain, and its resolution. This will influence the choice made for the width of the buffer zone and the weights of the blending and other factors that will be discussed later.

5. Comparison to global analyses

To remove the impact of boundary conditions, another assimilation experiment has been done in which global analyses were produced with a global version of CRCM5, referred to as GEMCLIM. The horizontal resolution of GEMCLIM is ~ 50 km; it has the same vertical discretization as the regional configuration, and the height of the top level is also the same. The global and regional model versions use the same lower boundary conditions. Sea ice cover and sea surface temperature are prescribed from ERA-Interim reanalyses while snow cover and thickness as well as sea ice thickness are produced by the model. This experiment will be taken as a reference to assess the impact of imposing lateral boundary conditions.

The variational assimilation is also very similar because the regional model benefits from the incremental formulation of the global assimilation. They both use the same observations (albeit limited to those within the domain of the CRCM5 for the regional assimilation) and the same observation and background error statistics. They only differ by the fact that different models are used to produce their own respective forecasts to evaluate the departures between observations and the background state. Over the CRCM5 domain, the mean global analysis increments for temperature (not shown)

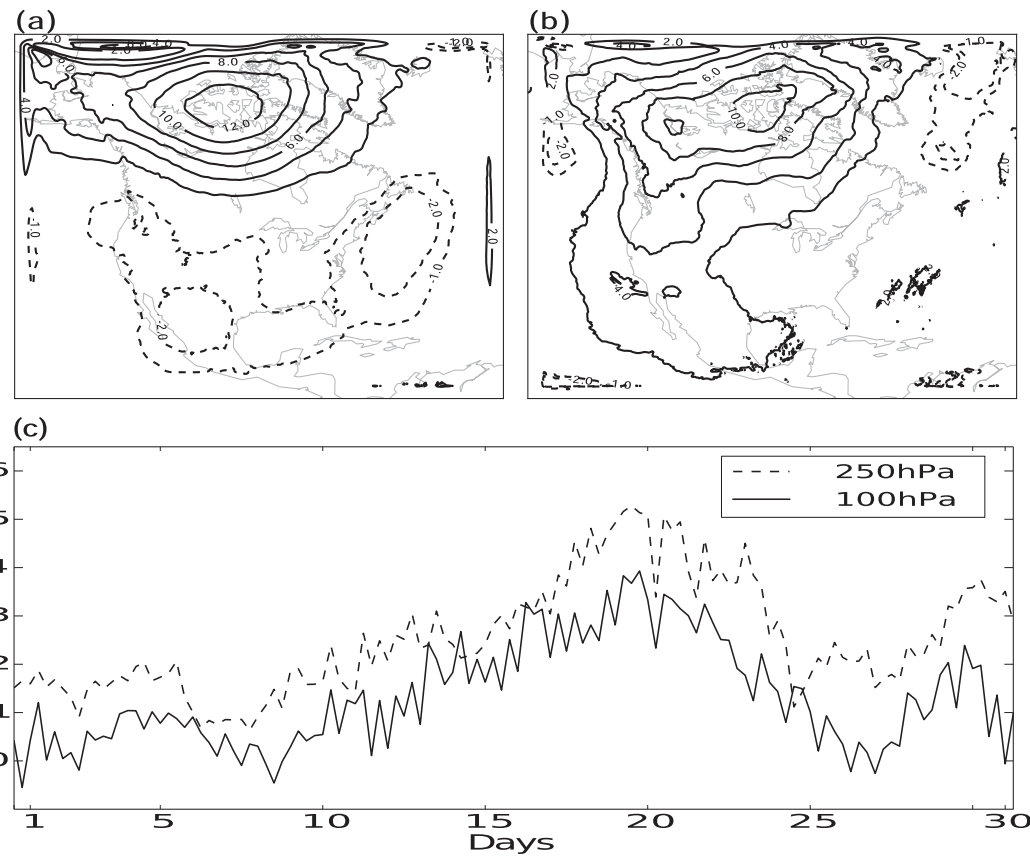


FIG. 6. Mean temperature initial systematic tendency related to dynamics (K day^{-1}) computed for the month of January 2011 at levels (a) 100 and (b) 250 hPa. (c) The temporal evolution of temperature tendency due to advection (K day^{-1}) for the month of January 2011 at levels 100 (solid line) and 250 hPa (dotted line).

do not have a similar bias to what was obtained with the regional experiment (see Fig. 2a). In addition, for the same set of radiosondes used before (Fig. 3), the monitoring for this experiment (not shown) indicates small mean OMF and OMA. The large bias seen before is absent. In this case, the model forecast is closer to the observations.

Figure 9 presents the initial mean temperature tendencies associated with global forecasts based on the global analyses. To compare with the results of the regional analyses and forecasts, the global tendencies have been averaged over the CRCM5 free zone. The process tendencies, especially those for dynamics, are much smaller than what was observed before (Fig. 5). In this case, the mean total tendency, as well as that from dynamics, is much more realistic and similar to results obtained in Chikhar and Gauthier (2014) for instance. In other words, the dynamical balance is realistic in the northern region contrary to what had been noted in the regional case.

Since the global assimilation uses a model that is very similar to the CRCM5, these results indicate that problems experienced in the regional case for January can unambiguously be attributed to the lateral boundary

conditions. It should be mentioned that the GEMCLIM analyses have a similar resolution as that of ERA-Interim but a higher vertical resolution (80 levels instead of 37) with a top level at 0.1 hPa (instead of 1 hPa). Referring to Chikhar and Gauthier (2014), this could have an impact on the total tendency. An experiment with the CRCM5 driven by GEMCLIM global analyses led to nearly the same results (large biases). Using the GEMCLIM global analyses instead of ERA-Interim analyses as driving data every 6 h, did not solve the problem.

The differences between the regional and global mean analysis increments could then be due to the treatment of boundary conditions to match two models that differ in terms of spatial resolution or physical parameterizations (Warner et al. 1997; Davies 2014).

6. Sensitivity to the extension of the domain and the nesting configuration

Several studies have shown that the boundary conditions can lead to problems associated with the nesting

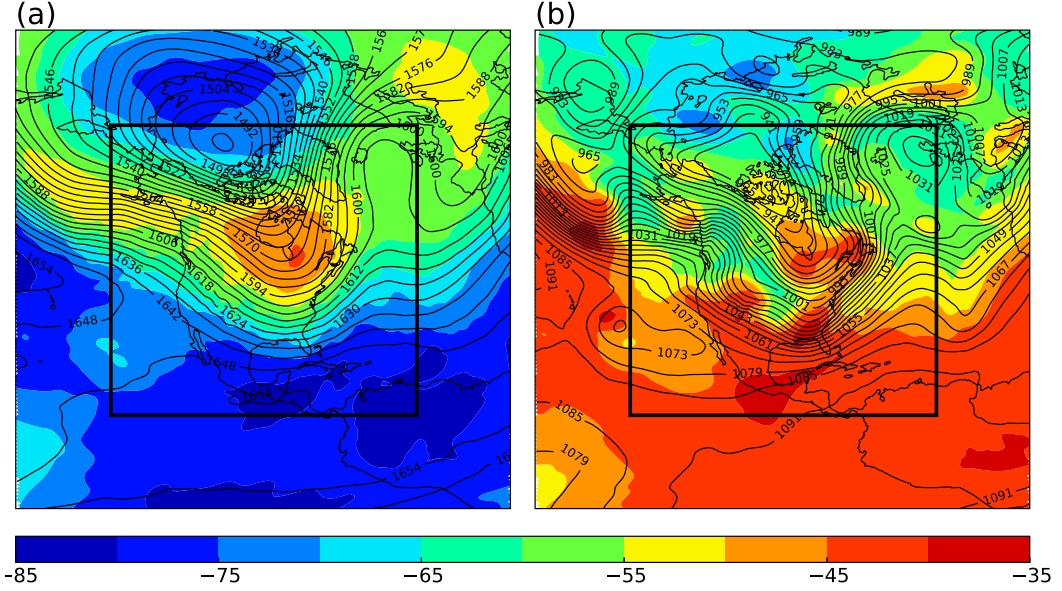


FIG. 7. Geopotential height (contours) and temperature (shaded colors) from ERA-Interim reanalysis valid at 1800 UTC 22 Jan for levels (a) 100 and (b) 250 hPa. The rectangular frame corresponds the CRCM5 model domain.

scheme, the size of the domain, and/or the position of the frontiers (Davies 2014; Fillion et al. 2010; Warner et al. 1997; Baumhefner and Perkey 1982). A strategy used for regional NWP forecasts is to extend the domain to move the boundary farther away from the domain of interest to avoid the problem at the boundaries impacting 48-h regional forecasts. This was tested in an experiment using all observations for January 2011 in which the domain was extended farther north and west.

Figure 10 covers the extended domain and shows that the mean analysis increments resulting from this experiment still have large negative values and similar patterns as those obtained with the regular domain. The monitoring for January 2011 of the same radiosondes as before (Fig. 11) still shows large departures between observations and the forecast but at a different time than before, suggesting that inconsistencies between the driving data and the regional model remain. Strong

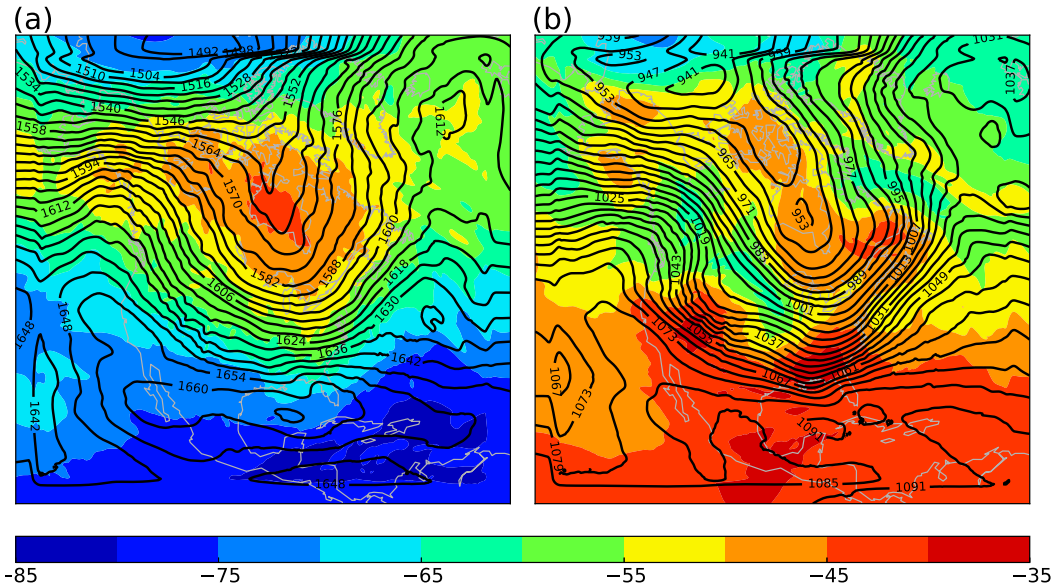


FIG. 8. As in Fig. 7, but for the 6-h regional forecast.

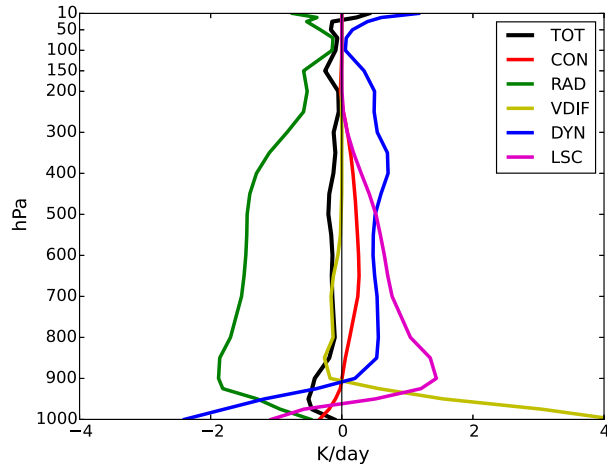


FIG. 9. Mean initial tendencies (K day^{-1}) from the global model averaged over the CRCM5 free zone. Colors coding is the same as in Fig. 5.

cross-boundary flows similar to those shown in Fig. 8 still occur through the northern boundary of the extended domain but not at the same time and location.

Figure 12 shows the corresponding tendency diagnostics that, as before (see Fig. 5), indicate a similar problem in the mean dynamics component of the temperature tendency. The results of this experiment show that increasing the size of the domain, at least in the way it was done here, did not correct the blending issue across the northern polar region in the presence of intermittent nonzonal large circulations prevailing in the boreal winter.

Finally, as pointed out in Zhong et al. (2010), another factor that can also impact the forecast in limited-area

models could be the size of the blending zone, where the solution from the regional model is relaxed toward the driving data. This was also tested by extending the blending zone from 10 to 20 grid points, but this did not change significantly the results that were almost identical.

7. Treatment of boundary conditions in the presence of rapidly changing cross-boundary flows

During the boreal winter, the large-scale circulation over the polar region can evolve rapidly over 6 h. Warner et al. (1997) and Denis et al. (2002) pointed out that the nesting scheme should allow a limited-area model to correctly handle such rapidly changing large-scale circulations. Up to now in our experiments, following what is currently done in CRCM5 climate simulations, the regional model was driven 6-hourly by global analyses for winds, temperature, specific humidity, and surface pressure with a linear temporal interpolation to intermediate time steps. A possible improvement in the nesting procedure could be obtained by more frequently refreshing the lateral boundary conditions.

Moreover, large-scale dynamics are not efficiently resolved in limited-area models when forced solely at the lateral boundaries and can conflict with the global driving data (von Storch et al. 2000). Systematic large-scale errors can also develop within the regional domain when using only the classic lateral nesting procedure (Kanamaru and Kanamitsu 2007). It is then preferable to constrain the large scales to those of the global

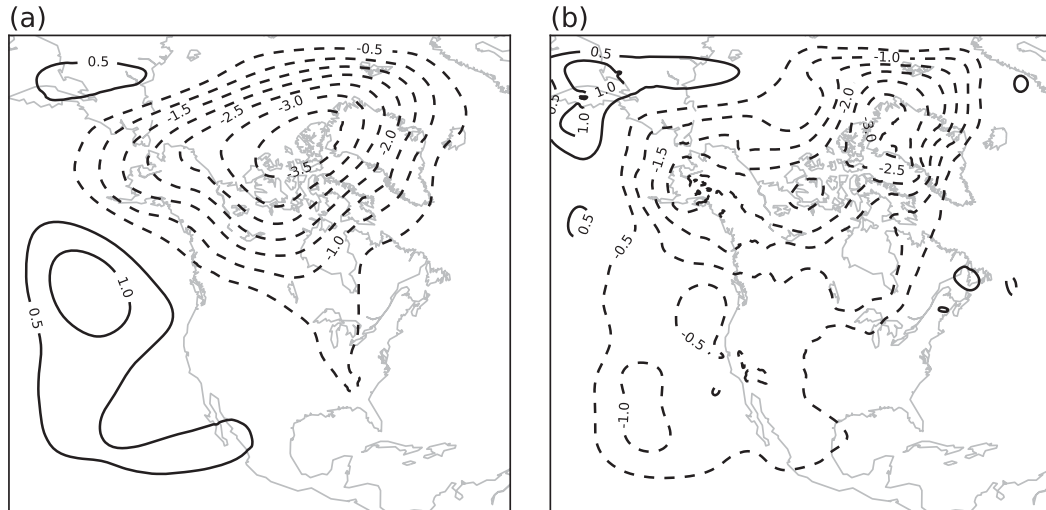


FIG. 10. Mean temperature increment from the analysis computed for January 2011 over the extended model domain for levels (a) 100 and (b) 250 hPa.

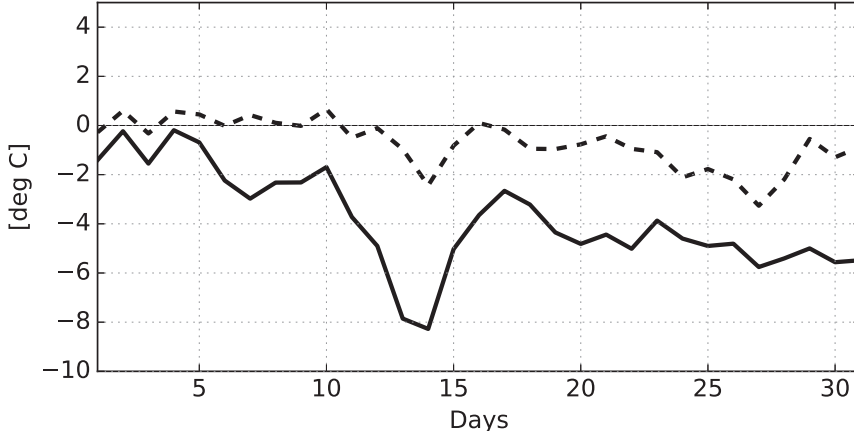


FIG. 11. Monitoring of the radiosondes at 100 hPa as in Fig. 4 for the experiment with the extended domain for January 2011.

analyses or forecasts from a global circulation model sharing the same physics and dynamics as the regional model (Scinocca et al. 2016). This can be done by imposing a so-called *spectral nudging* that can help prevent decoupling between the regional climate internal solution and the lateral forcing data (Gustafsson et al. 1998; Miguez-Macho et al. 2004; Alexandru et al. 2009; Glisan et al. 2013; Scinocca et al. 2016). Large-scale spectral nudging is a restoring force applied over the entire domain toward the prescribed large-scale components of the driving global model.

The sensitivity to the temporal resolution of the lateral boundary conditions was first examined by increasing the frequency at which these are updated. The GEMCLIM global analyses and forecasts have been used because they can provide the information needed for the boundary conditions up to every time step to drive the CRCM5. Moreover, this also provides consistency between the two models and reduces the difference in spatial resolution between the regional model and the driving data as recommended in Davies (2014) and Warner et al. (1997). It is recalled that GEMCLIM global analyses and forecasts are produced at a ~ 50 -km horizontal resolution and on the same 80 vertical levels as in the CRCM5. On the other hand, ERA-Interim does not provide analyses at a similar vertical resolution and are only available at 6-h intervals.

The first experiment consisted of comparing the mean analysis increments for the period of January 2011 obtained by updating the boundary conditions every 6 h to those obtained when updating these boundary conditions at the highest temporal frequency, that is, every time step (10 min). Figures 13a and 13b indicate that this has reduced the bias in the analysis increments at 100 hPa (top panels) and 250 hPa (bottom panels). If, on

top of updating the boundary conditions at every time step, a spectral nudging constraint is added with a relaxation time of 24 h, then this has an additional positive impact as shown in Fig. 13c. Figure 14 shows the results of the monitoring for the same radiosondes as before. When the model is driven at each time step without spectral nudging (blue lines), the decrease in the OMF mean values is nearly 4 K during the period 18–24 January. Adding the spectral nudging (green lines) decreases the temperature bias by about 1 K at its peak, but has little impact outside this period.

In Davies (2014), it is shown that the lateral boundaries conditions should be updated more frequently than at every 6 h as is currently done in the CRCM5. This suggests to test the impact of the frequency of the updates in experiments in which the lateral forcing was updated every 6, 3, 1 h, and finally, at every time step

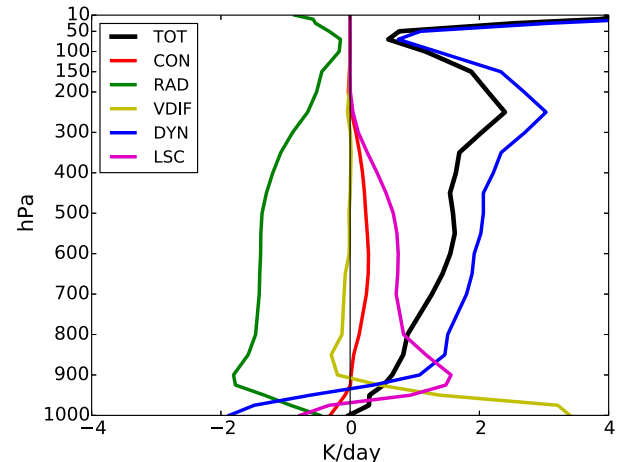


FIG. 12. As in Fig. 5, but for CRCM5 extended domain experiment.

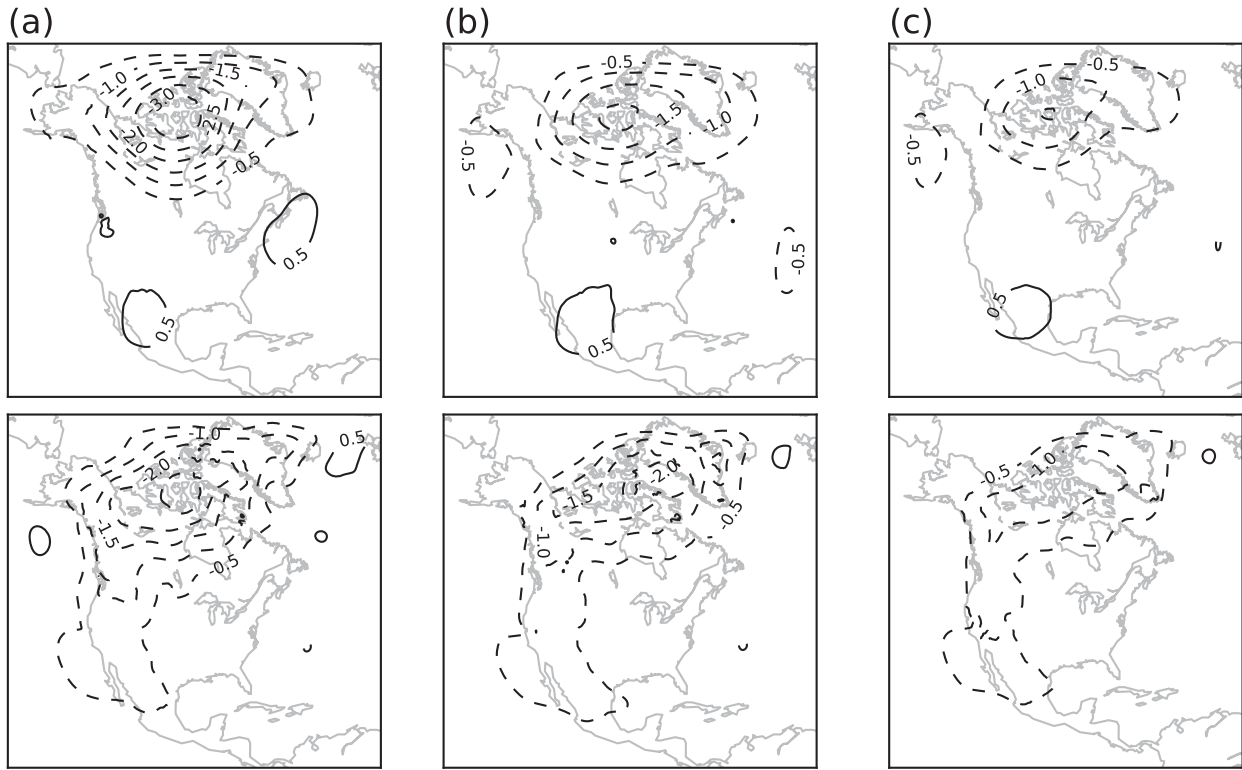


FIG. 13. Mean temperature analysis increment (K) computed for January 2011 at (top) 100- and (bottom) 250-hPa levels when CRCM5 is laterally driven using different nesting strategies. (a) CRCM5 is driven 6-hourly by GEMCLIM global analyses; (b) CRCM5 is driven every time step by GEMCLIM global analyses and forecasts; and (c) as in (b), with additional spectral nudging applied with a relaxation time of 24 h.

applying also a spectral nudging constraint with a 24-h relaxation time. Figures 15 and 16 show, respectively, the mean increments and the data monitoring obtained from these experiments showing a clear improvement

when increasing the frequency. The most significant improvement is obtained when the temporal frequency is increased from 6 to 3 h, but it is minimal when increasing the frequency from 1 h to each time step (blue

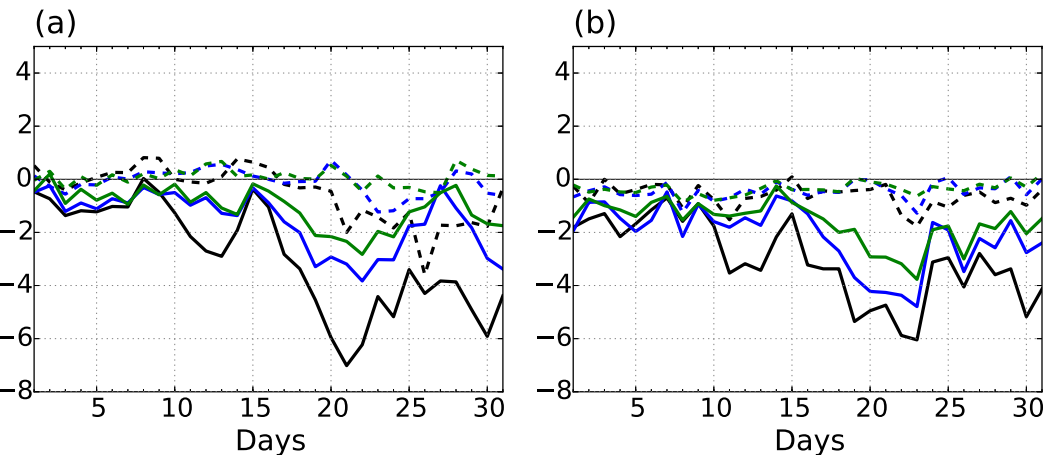


FIG. 14. Mean OMF (solid lines) and OMA (dotted lines) for temperature (K) from radiosondes shown in Fig. 3 for January 2011 at (a) 100 and (b) 250 hPa. Results from cycles where CRCM5 is driven 6-hourly (black), every time step (blue), and every time step with spectral nudging (green) (applied with a relaxation time of 24 h) are presented.

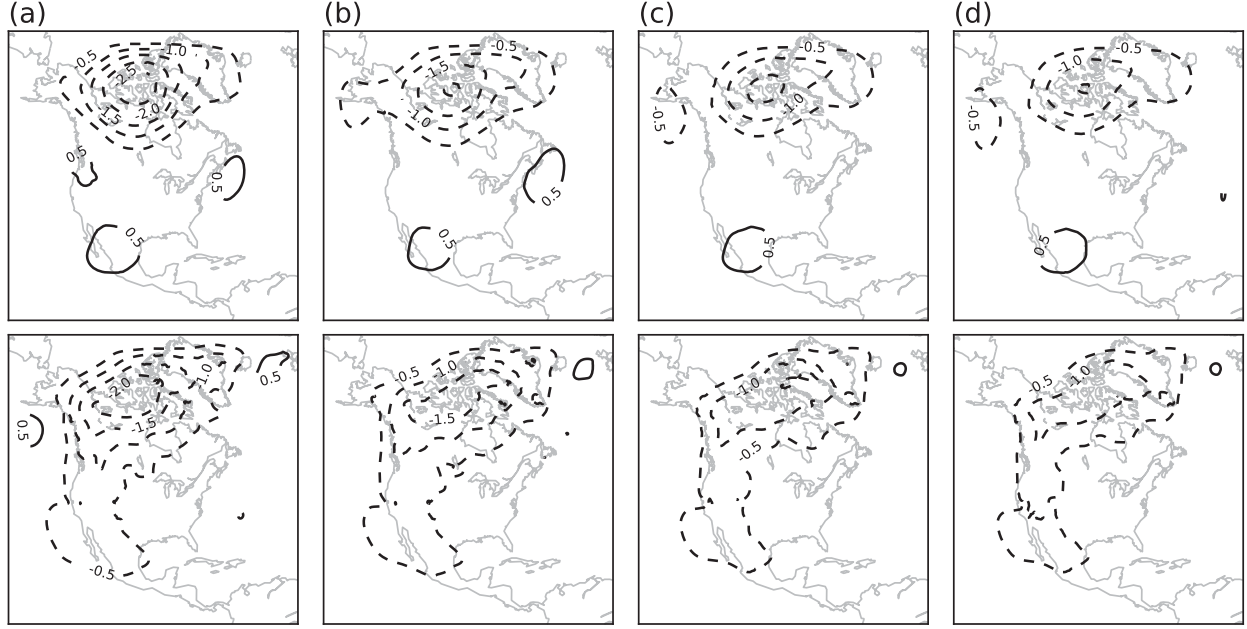


FIG. 15. As in Fig. 13, but where CRCM5 is driven by GEMCLIM global analyses and forecasts (a) 6-hourly, (b) 3-hourly, (c) hourly, and (d) every time step. Spectral nudging is applied in each case with a 24-h relaxation time.

and black lines in Fig. 16). Given that the time step is 10 min, it would be a significant savings in computing time if updating is done only every hour. These results show that the impact of doing so would be minimal.

The other factor that was introduced is a constraint on the large scales through spectral nudging applied to wind and temperature. As in Scinocca et al. (2016), the spectral nudging is only applied to scales larger than about 400 km, over the whole column with a maximal strength between the model top and 0.85 hybrid model level (~ 850 hPa). Below 850 hPa, the spectral nudging

strength is decreased through a squared cosine profile and becomes null at the lowest model level. The strength of the spectral nudging is defined by the relaxation time and, in these experiments, was decreased from 16 to 6 h, where the shorter the relaxation time, the stronger the constraint on the large scales. The boundary conditions were updated at every time step in all cases. The results of Figs. 17 and 18 show that increasing the strength of the spectral nudging (shorter relaxation times) leads to a gradual decrease in the mean analysis increments and the observations departures (OMF and OMA).

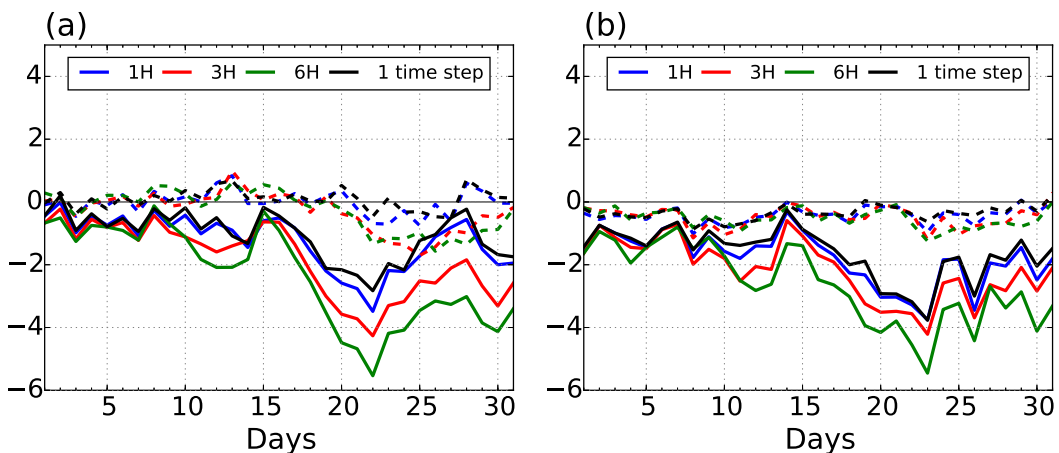


FIG. 16. As in Fig. 14, but where CRCM5 is driven by GEMCLIM global analyses and forecasts 6-hourly (green), 3-hourly (red), hourly (blue), and at every time step (black). Spectral nudging is applied in each case with a 24-h relaxation time.

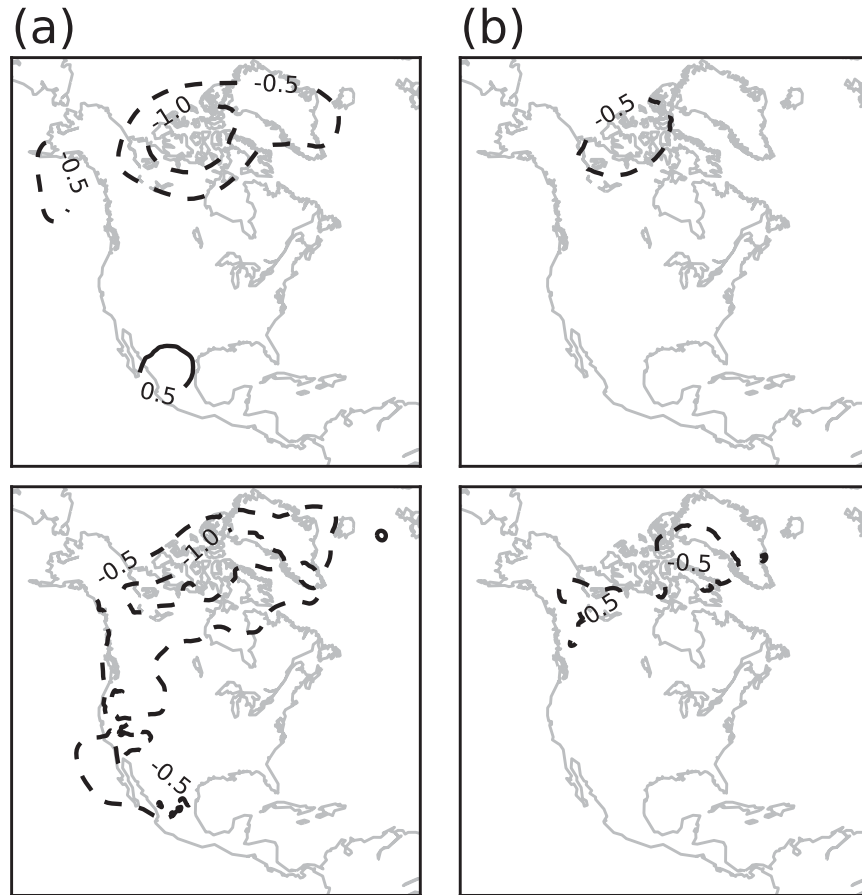


FIG. 17. As in Fig. 13, but where CRCM5 is driven by GEMCLIM global analyses and forecasts each time step with spectral nudging applied at (a) 1% and (b) 2.8% corresponding to a relaxation time of ~ 16 and 6 h, respectively.

Moreover, comparing the analysis increments (Figs. 17a and 17b) and the corresponding results for monitoring (red and green lines in Fig. 18) reveals that the improvement is most significant when the relaxation time is decreased from 16 to 6 h.

8. Verification of the adopted configuration

Based on the results of the previous experiments using a 24-h relaxation time for the spectral nudging, increasing the lateral driving frequency from 1 h to one time step does not seem to bring significant improvements. This motivates our choice of updating the driving data at 1-h intervals to reduce the computational cost. This is also what is used in the regional data assimilation of the Meteorological Service of Canada (Fillion et al. 2010). As for spectral nudging, results with updating the driving data at every time step showed that setting the relaxation time to 6 h in the spectral nudging has a significant positive impact considerably reducing the

boundary decoupling. This is our justification for testing a configuration with hourly lateral driving combined with a spectral nudging with a 6-h relaxation time.

This was tested in a data assimilation cycle for January 2011. The resulting mean increment is very similar to what is obtained when the model is driven at each time step (Fig. 17b) confirming the fact that the hourly temporal frequency is high enough to enable the CRCM5 to correctly interact with the driving data. Data monitoring (Fig. 19) yields also very similar observation departures (OMF and OMA) for these two cycles. This configuration therefore constitutes a good compromise between the lateral decoupling minimization and computing cost as well as data storage.

The initial tendency diagnostic has been computed for January 2011, and Fig. 20 shows that the mean total temperature tendency profile (black line) has a much better behavior than that shown in Fig. 5 for our original configuration driven 6-hourly using ERA-Interim reanalyses without spectral nudging. Moreover, the

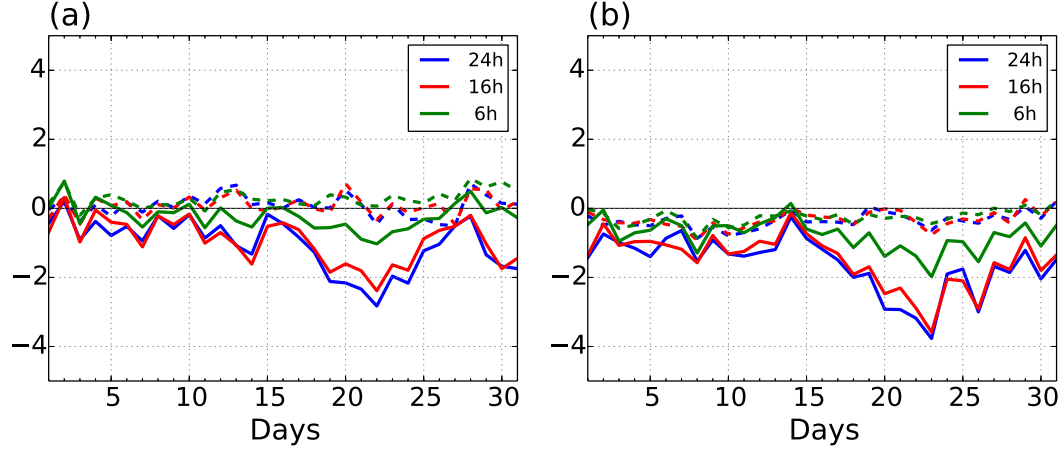


FIG. 18. As in Fig. 14, but where CRCM5 is driven by GEMCLIM global analyses and forecasts each time step with spectral nudging applied with a relaxation time of ~ 16 (red) and 6 h (green). Blue lines are identical to black lines in Fig. 16 and are added for comparison purpose.

synoptic circulation for the same date as in Fig. 8 is presented in Fig. 21. It shows a much better transition near the northern boundary, and the decoupling through the blending zone has almost disappeared. In this case, the circulation is very similar to what is observed in the global analyses (Fig. 7). In the original configuration, the mismatch between the lateral boundary conditions and the different evolution in the limited-area model reduced the transport of cold air in the interior of the domain to create important departures between the background state and the observations. This new nesting strategy leads to a better agreement of the model evolution with the lateral boundary conditions.

Figures 2 and 4 indicated that the problems with the regional analyses were more acute at upper levels than in the lower part of the atmosphere. However, as surface

temperatures are of particular interest for regional climate studies, the bias and rms error were evaluated for 2-m background and analysis temperature with respect to surface observations for January and July 2011. Figure 22 indicates that the model has a small negative bias around -1 K in July, while in January the bias is more variable, exhibiting a trend from about -1 up to 0 K.

Figure 23 presents the rms errors and biases for 6-h forecasts (OMF) and analyses (OMA) for temperature with respect to radiosonde observations. The OMF (Figs. 23a,b) has lower biases and rms errors in July while, in January, they are both higher above 250 hPa. However, a comparison with the results obtained with the original configuration (dotted lines in Figs. 23a,b) indicates a significant improvement. As expected, the

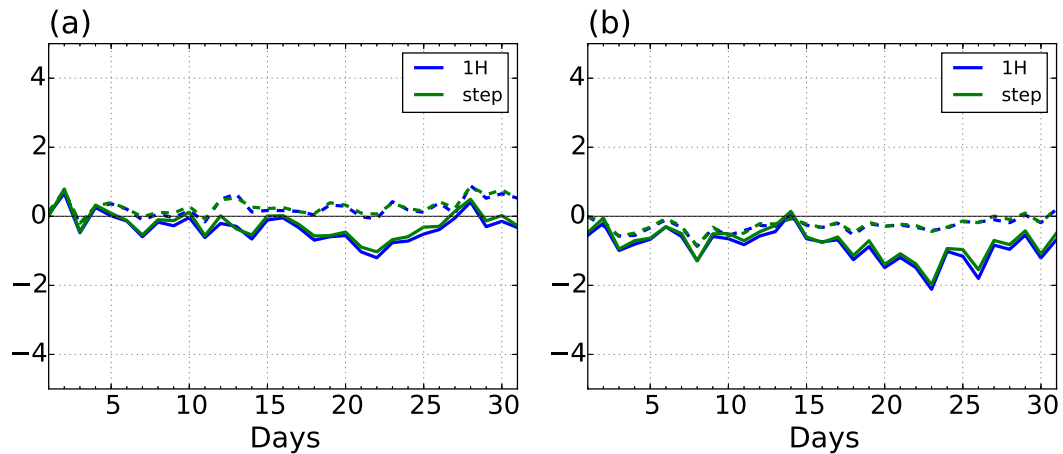


FIG. 19. As in Fig. 14, but where CRCM5 is driven hourly (blue) and each time step (green) by GEMCLIM global analyses and forecasts with spectral nudging applied with a 6-h relaxation time.

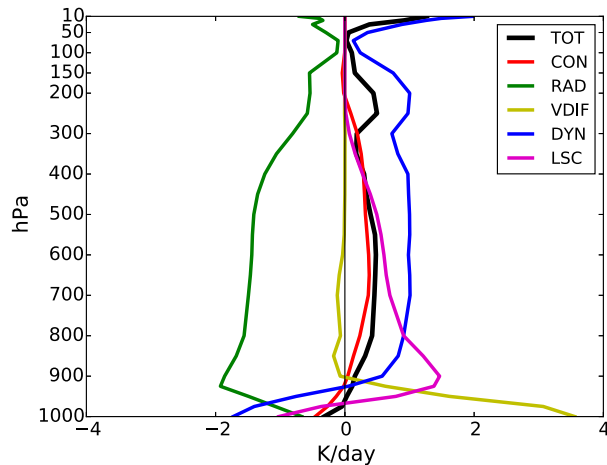


FIG. 20. As in Fig. 5, but for January cycle using the adopted lateral driving strategy (see text for details).

biases and rms errors are also lower for the OMA (Figs. 23c,d).

9. Conclusions

The main motivation for using CRCM5 forecasts as background states for data assimilation was to evaluate this regional climate model. Following RP07, biases in the analysis increments can be related to the initial tendencies that provide information to identify the source of such systematic differences if related to physical processes acting on fast time scales in the model. Several assimilation cycles were completed over

two months, January and July 2011. As currently done in regional climate simulations with the CRCM5, the lateral boundary conditions were prescribed every 6 h from ERA-Interim reanalyses. In January, the mean increments had a large negative bias particularly at higher levels in the northern part of the domain. The monitoring of temperature observations from radiosondes (OMF) in this region detected important systematic departures of the model's forecasts associated with a particular period during which there were cross-boundary flows and strong temperature gradients.

Diagnostics based on mean initial temperature tendencies revealed an abnormal tendency associated with advection of temperature, particularly in the northern part of the model's domain. This occurred when very strong winds are crossing through the northern lateral boundary creating a mismatch between ERA-Interim driving data and the CRCM5 forecast in the interior. Since this does not occur in global analyses produced with the global version of the CRCM5, this experiment enabled us to focus on the treatment of the lateral boundary conditions in the model.

According to studies in the literature, the problem could be solved by extending the domain, more frequently updating the boundary conditions, and/or constraining the large scales in the interior of the limited-area model. The results obtained by extending the domain north and west did not solve the problem as the large-scale nonzonal circulations that often prevail in the Arctic region in winter still created cross-boundary flows that did not match the evolution of the

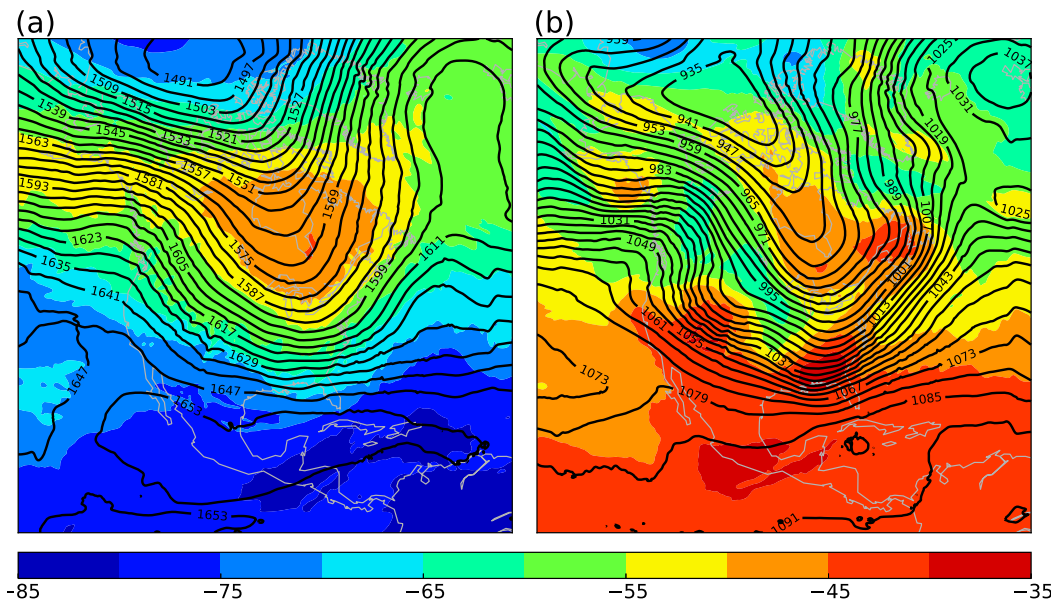


FIG. 21. As in Fig. 8, but for CRCM5 driven hourly with additional spectral nudging with a 6-h relaxation time.

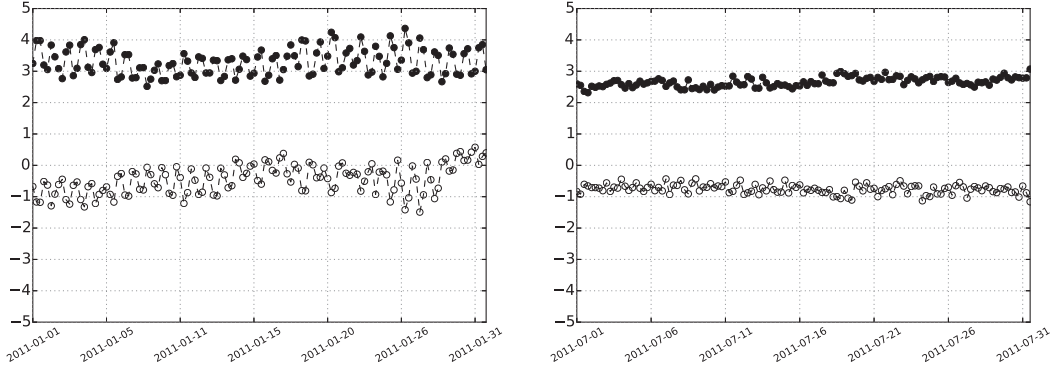


FIG. 22. Bias (hollow circles) and rms (black dots) for the background 2-m temperatures for (left) January 2011 and (right) July 2011.

CRCM5. However, the data monitoring indicated that the problem occurred over a different period and different region when strong cross-boundary flows occurred through the northern boundary. The diagnostics

of the temperature tendency confirmed that it was still the tendency associated with temperature advection that led to a biased total temperature tendency. The impact of increasing the updating frequency was tested

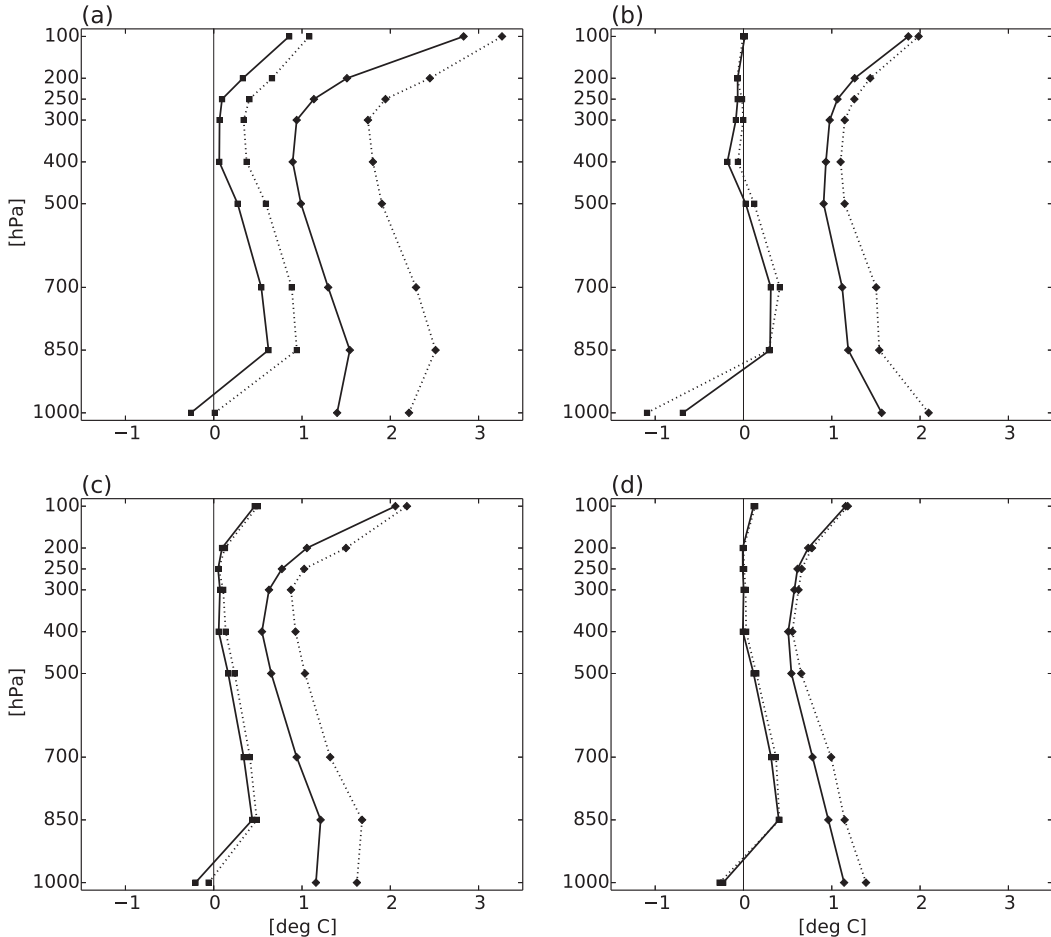


FIG. 23. Bias (squares) and rms (diamonds) for (a), (b) first-guess and (c), (d) analysis temperature fits to radiosonde observations for (left) January 2011 and (right) July 2011. Dotted lines represent results from cycles where CRCM5 is 6-hourly driven by ERA-Interim reanalyses.

for the period of January, reducing the update time interval down to every time step. Significant improvements were obtained by increasing the updating frequency down to every hour, but no significant gain could be measured by decreasing further.

Furthermore, in von Storch et al. (2000), it is suggested that a constraint on the large scales over the whole domain should be imposed to keep them close to the global data from analyses. This can be done with a technique called spectral nudging, the intensity of which is measured by the relaxation time being used. The results showed that introducing the spectral nudging with a relaxation time of 6 h added to the gain obtained with a more frequent updating of the lateral boundary conditions. With an update frequency of 1 h and spectral nudging with a 6-h relaxation time, the bias in the analysis increments was substantially reduced. A comparison with respect to surface and radiosonde data showed that these changes reduced significantly, particularly for the period of January, but did not eliminate completely the bias and rms errors.

Validating models through a direct comparison to observations is certainly useful, and this is what data assimilation does first before correcting the forecast to bring it closer to observations. Monitoring observations can detect intermittent problems that may occur. The tendency diagnostics of RP07 are extremely useful and allowed us to relate the presence of a bias in the analysis increment to the treatment of the lateral boundary conditions. Moreover, they also proved useful in assessing the impact of proposed changes to address the problem. The magnitude of the reduction of the biases in the analysis increments provides certainly good evidence that the configuration of the model has to be changed in this manner to obtain reliable analyses. This is only but a first step and a more thorough evaluation is needed. Pursuing the assimilation over a longer period of time will be useful to obtain more cases that would confirm our findings based on just a few cases.

Acknowledgments. The authors thank Dr. Stéphane Laroche for his valuable comments and advice. We thank also Mr. Michel Valin, Mrs. Katja Winger, Drs. Bin He, Sylvain Heilliette, and Ping Du for their assistance at implementing the assimilation system on Compute Québec's high performance computing platform. Observation datasets used in the assimilation were provided by Environment and Climate Change Canada (ECCC). This work would not have been possible without having had access to the variational assimilation system developed and validated at ECCC. We also would like to thank the anonymous reviewers for their comments and suggestions that helped to improve the

manuscript. This research has been funded by the Grants and Contribution program of ECCC and a grant from the Natural Sciences and Engineering Research Council of Canada (NSERC) Discovery Grant program. We gratefully acknowledge additional support from the Canadian Network for Regional Climate and Weather Processes (CNRCWP) funded through NSERC's Climate Change and Atmosphere Research programme (CCAR). High performance computing resources were provided by Compute Canada on the Guillimin platform of the Calcul Québec regional consortium.

REFERENCES

- Alexandru, A., R. De Elia, R. Laprise, L. Šeparović, and S. Biner, 2009: Sensitivity study of regional climate model simulations to large-scale nudging parameters. *Mon. Wea. Rev.*, **137**, 1666–1686, doi:[10.1175/2008MWR2620.1](https://doi.org/10.1175/2008MWR2620.1).
- Baumhefner, D. P., and D. J. Perkey, 1982: Evaluation of lateral boundary errors in a limited-domain model. *Tellus*, **34A**, 409–428, doi:[10.1111/j.2153-3490.1982.tb01831.x](https://doi.org/10.1111/j.2153-3490.1982.tb01831.x).
- Buehner, M., and Coauthors, 2015: Implementation of deterministic weather forecasting systems based on ensemble-variational data assimilation at Environment Canada. Part I: The global system. *Mon. Wea. Rev.*, **143**, 2532–2559, doi:[10.1175/MWR-D-14-00354.1](https://doi.org/10.1175/MWR-D-14-00354.1).
- Caron, J.-F., T. Milewski, M. Buehner, L. Fillion, M. Reszka, S. Macpherson, and J. St-James, 2015: Implementation of deterministic weather forecasting systems based on ensemble-variational data assimilation at Environment Canada. Part II: The regional system. *Mon. Wea. Rev.*, **143**, 2560–2580, doi:[10.1175/MWR-D-14-00353.1](https://doi.org/10.1175/MWR-D-14-00353.1).
- Chikhar, K., and P. Gauthier, 2014: Impact of analyses on the dynamical balance of global and limited-area atmospheric models. *Quart. J. Roy. Meteor. Soc.*, **140**, 2535–2545, doi:[10.1002/qj.2319](https://doi.org/10.1002/qj.2319).
- , and —, 2015: On the effect of boundary conditions on the Canadian Regional Climate Model: Use of process tendencies. *Climate Dyn.*, **45**, 2515–2526, doi:[10.1007/s00382-015-2488-2](https://doi.org/10.1007/s00382-015-2488-2).
- Côté, J., S. Gravel, A. Méthot, A. Patoine, M. Roch, and A. Staniforth, 1998: The operational CMC-MRB Global Environmental Multiscale (GEM) model. Part I: Design considerations and formulation. *Mon. Wea. Rev.*, **126**, 1373–1395, doi:[10.1175/1520-0493\(1998\)126<1373:TOCMGE>2.0.CO;2](https://doi.org/10.1175/1520-0493(1998)126<1373:TOCMGE>2.0.CO;2).
- Courtier, P., J.-N. Thépaut, and A. Hollingsworth, 1994: A strategy for operational implementation of 4D-Var, using an incremental approach. *Quart. J. Roy. Meteor. Soc.*, **120**, 1367–1387, doi:[10.1002/qj.49712051912](https://doi.org/10.1002/qj.49712051912).
- Davies, H., 1976: A lateral boundary formulation for multi-level prediction models. *Quart. J. Roy. Meteor. Soc.*, **102**, 405–418, doi:[10.1002/qj.49710243210](https://doi.org/10.1002/qj.49710243210).
- Davies, T., 2014: Lateral boundary conditions for limited area models. *Quart. J. Roy. Meteor. Soc.*, **140**, 185–196, doi:[10.1002/qj.2127](https://doi.org/10.1002/qj.2127).
- Dee, D. P., 2005: Bias and data assimilation. *Quart. J. Roy. Meteor. Soc.*, **131**, 3323–3343, doi:[10.1256/qj.05.137](https://doi.org/10.1256/qj.05.137).
- , and Coauthors, 2011: The ERA-Interim reanalysis: Configuration and performance of the data assimilation system. *Quart. J. Roy. Meteor. Soc.*, **137**, 553–597, doi:[10.1002/qj.828](https://doi.org/10.1002/qj.828).
- Denis, B., R. Laprise, D. Caya, and J. Côté, 2002: Downscaling ability of one-way nested regional climate models: The Big-Brother experiment. *Climate Dyn.*, **18**, 627–646, doi:[10.1007/s00382-001-0201-0](https://doi.org/10.1007/s00382-001-0201-0).

- Fillion, L., and Coauthors, 2010: The Canadian Regional Data Assimilation and Forecasting System. *Wea. Forecasting*, **25**, 1645–1669, doi:[10.1175/2010WAF2222401.1](https://doi.org/10.1175/2010WAF2222401.1).
- Gauthier, P., C. Chouinard, and B. Brasnett, 2003: Quality control: Methodology and applications. *Data Assimilation for the Earth System*, R. Swinbank, V. Shutyaev, and W. A. Lahoz, Eds., Springer, 177–187, doi:[10.1007/978-94-010-0029-1_15](https://doi.org/10.1007/978-94-010-0029-1_15).
- , M. Tanguay, S. Laroche, S. Pellerin, and J. Morneau, 2007: Extension of 3DVAR to 4DVAR: Implementation of 4DVAR at the Meteorological Service of Canada. *Mon. Wea. Rev.*, **135**, 2339–2354, doi:[10.1175/MWR3394.1](https://doi.org/10.1175/MWR3394.1).
- Gilbert, J. C., and C. Lemaréchal, 1989: Some numerical experiments with variable-storage quasi-Newton algorithms. *Math. Programm.*, **45**, 407–435, doi:[10.1007/BF01589113](https://doi.org/10.1007/BF01589113).
- Glisan, J. M., W. J. Gutowski Jr., J. J. Cassano, and M. E. Higgins, 2013: Effects of spectral nudging in WRF on arctic temperature and precipitation simulations. *J. Climate*, **26**, 3985–3999, doi:[10.1175/JCLI-D-12-00318.1](https://doi.org/10.1175/JCLI-D-12-00318.1).
- Gustafsson, N., E. Källén, and S. Thorsteinsson, 1998: Sensitivity of forecast errors to initial and lateral boundary conditions. *Tellus*, **50A**, 167–185, doi:[10.1034/j.1600-0870.1998.t01-1-00002.x](https://doi.org/10.1034/j.1600-0870.1998.t01-1-00002.x).
- Houtekamer, P. L., X. Deng, H. L. Mitchell, S.-J. Baek, and N. Gagnon, 2014: Higher resolution in an operational ensemble Kalman filter. *Mon. Wea. Rev.*, **142**, 1143–1162, doi:[10.1175/MWR-D-13-00138.1](https://doi.org/10.1175/MWR-D-13-00138.1).
- Kanamaru, H., and M. Kanamitsu, 2007: Scale-selective bias correction in a downscaling of global analysis using a regional model. *Mon. Wea. Rev.*, **135**, 334–350, doi:[10.1175/MWR3294.1](https://doi.org/10.1175/MWR3294.1).
- Laprise, R., 1992: The Euler equations of motion with hydrostatic pressure as an independent variable. *Mon. Wea. Rev.*, **120**, 197–207, doi:[10.1175/1520-0493\(1992\)120<0197:TEEOMW>2.0.CO;2](https://doi.org/10.1175/1520-0493(1992)120<0197:TEEOMW>2.0.CO;2).
- Laroche, S., P. Gauthier, J. St-James, and J. Morneau, 1999: Implementation of a 3D variational data assimilation system at the Canadian Meteorological Centre. Part II: The regional analysis. *Atmos.–Ocean*, **37**, 281–307, doi:[10.1080/07055900.1999.9649630](https://doi.org/10.1080/07055900.1999.9649630).
- , —, M. Tanguay, S. Pellerin, and J. Morneau, 2007: Impact of the different components of 4DVAR on the Global Forecast System of the Meteorological Service of Canada. *Mon. Wea. Rev.*, **135**, 2355–2364, doi:[10.1175/MWR3408.1](https://doi.org/10.1175/MWR3408.1).
- Mailhot, J., and Coauthors, 2006: The 15-km version of the Canadian Regional Forecast System. *Atmos.–Ocean*, **44**, 133–149, doi:[10.3137/ao.440202](https://doi.org/10.3137/ao.440202).
- Mesinger, F., and Coauthors, 2006: North American Regional Reanalysis. *Bull. Amer. Meteor. Soc.*, **87**, 343–360, doi:[10.1175/BAMS-87-3-343](https://doi.org/10.1175/BAMS-87-3-343).
- Miguez-Macho, G., G. L. Stenchikov, and A. Robock, 2004: Spectral nudging to eliminate the effects of domain position and geometry in regional climate model simulations. *J. Geophys. Res.*, **109**, D13104, doi:[10.1029/2003JD004495](https://doi.org/10.1029/2003JD004495).
- Parrish, D. F., and J. C. Derber, 1992: The National Meteorological Center's spectral statistical-interpolation analysis system. *Mon. Wea. Rev.*, **120**, 1747–1763, doi:[10.1175/1520-0493\(1992\)120<1747:TNCSS>2.0.CO;2](https://doi.org/10.1175/1520-0493(1992)120<1747:TNCSS>2.0.CO;2).
- Rodwell, M. J., and T. N. Palmer, 2007: Using numerical weather prediction to assess climate models. *Quart. J. Roy. Meteor. Soc.*, **133**, 129–146, doi:[10.1002/qj.23](https://doi.org/10.1002/qj.23).
- , and T. Jung, 2008: Understanding the local and global impacts of model physics changes: An aerosol example. *Quart. J. Roy. Meteor. Soc.*, **134**, 1479–1497, doi:[10.1002/qj.298](https://doi.org/10.1002/qj.298).
- Scinocca, J., and Coauthors, 2016: Coordinated global and regional climate modeling. *J. Climate*, **29**, 17–35, doi:[10.1175/JCLI-D-15-0161.1](https://doi.org/10.1175/JCLI-D-15-0161.1).
- Separović, L., A. Alexandru, R. Laprise, A. Martynov, L. Sushama, K. Winger, K. Tete, and M. Valin, 2013: Present climate and climate change over North America as simulated by the fifth-generation Canadian regional climate model. *Climate Dyn.*, **41**, 3167–3201, doi:[10.1007/s00382-013-1737-5](https://doi.org/10.1007/s00382-013-1737-5).
- von Storch, H., H. Langenberg, and F. Feser, 2000: A spectral nudging technique for dynamical downscaling purposes. *Mon. Wea. Rev.*, **128**, 3664–3673, doi:[10.1175/1520-0493\(2000\)128<3664:ASNTFD>2.0.CO;2](https://doi.org/10.1175/1520-0493(2000)128<3664:ASNTFD>2.0.CO;2).
- Warner, T. T., R. A. Peterson, and R. E. Treadon, 1997: A tutorial on lateral boundary conditions as a basic and potentially serious limitation to regional numerical weather prediction. *Bull. Amer. Meteor. Soc.*, **78**, 2599–2617, doi:[10.1175/1520-0477\(1997\)078<2599:ATOLBC>2.0.CO;2](https://doi.org/10.1175/1520-0477(1997)078<2599:ATOLBC>2.0.CO;2).
- Zadra, A., D. Caya, J. Côté, B. Dugas, C. Jones, R. Laprise, K. Winger, and L.-P. Caron, 2008: The next Canadian regional climate model. *Phys. Can.*, **64**, 75–83.
- Zhong, Z., X. Wang, W. Lu, and Y. Hu, 2010: Further study on the effect of buffer zone size on regional climate modeling. *Climate Dyn.*, **35**, 1027–1038, doi:[10.1007/s00382-009-0662-0](https://doi.org/10.1007/s00382-009-0662-0).